HHS Public Access

Author manuscript

Toxicol Lett. Author manuscript; available in PMC 2023 February 01.

Published in final edited form as:

Toxicol Lett. 2023 February 01; 374: 31–39. doi:10.1016/j.toxlet.2022.11.021.

Tris(1,3-dichloro-2-propyl) phosphate is a metabolism-disrupting chemical in male mice

Sara Y. Ngo Tenlep[a], **Megan Weaver**[a], **Jianzhong Chen**[b], **Olga Vsevolozhskaya**[c], **Andrew J. Morris**[b,d], **Cetewayo S. Rashid**[a,e,*]

[a]Department of Pharmacology and Nutritional Sciences, University of Kentucky, Lexington, KY, USA

[b]Division of Cardiovascular Medicine, University of Kentucky College of Medicine, Lexington, KY, USA

[c]Department of Biostatistics, University of Kentucky, Lexington, KY, USA

[d]Lexington Veterans Affairs Healthcare System, Lexington, KY, USA

[e]Barnstable Brown Diabetes and Obesity Center, University of Kentucky, Lexington, KY, USA

Abstract

Tris(1,3-dichloro-2-propyl) phosphate (TDCPP) is an organophosphate flame retardant. The primary TDCPP metabolite, bis(1,3-dichloro-2-propyl) phosphate (BDCPP), is detectable in the urine of over 90 % of Americans. Epidemiological studies show sex-specific associations between urinary BDCPP levels and metabolic syndrome, which is an established risk factor for type 2 diabetes, heart disease, and stroke. We used a mouse model to determine whether TDCPP exposure disrupts glucose homeostasis. Six-week old male and female C57BL/6J mice were given ad libitum access to diets containing vehicle (0.1 % DMSO) and TDCPP resulting in the following treatment groups: 0 mg/kg/day, 0.02 mg/kg/day, 1 mg/kg/day, or 100 mg/kg/day. After being on the experimental diet for five weeks without interruption, body composition was analyzed, glucose and insulin tolerance tests were performed, and fasting glucose and insulin levels were quantified. TDCPP at 100 mg/kg/day caused male sex-specific adiposity, fasting hyperglycemia, and insulin resistance. TDCPP-induced modulation of nuclear receptor activation was investigated using an in vitro screen to identify potential mechanisms of metabolic disruption. TDCPP activated farnesoid X receptor (FXR) and pregnane X receptor (PXR), and inhibited the androgen receptor (AR). PXR target genes, but not FXR target genes, were upregulated in livers from mice exposed to 100 mg TDCPP/kg/day. Interestingly, PXR target genes were differentially expressed in livers from both males and females. It remains to be determined whether TDCPP-induced metabolic disruption occurs via modulation of nuclear receptor activity. Taken together, these studies build upon the

*Correspondence to: University of Kentucky, 900 S. Limestone St., 566C.T. Wethington Bldg., Lexington, KY 40536, USA. cetewayo.rashid@uky.edu (C.S. Rashid).

Declaration of Competing Interest

The authors declare that they have no known competing financial interests or personal relationships that could have appeared to influence the work reported in this paper.

Appendix A. Supporting information

Supplementary data associated with this article can be found in the online version at doi:10.1016/j.toxlet.2022.11.021.

association of TDCPP exposure and metabolic syndrome in humans by identifying sex-specific effects of TDCPP on glucose homeostasis in mice.

Keywords

Organophosphate flame retardant; TDCPP; Insulin resistance; Glucose tolerance; Body composition; Nuclear receptor

1. Introduction

Flame retardants have been used since the 1970′s to protect against fire losses, and subsequently the fire death rate in the U.S. has decreased 70 % (Ahrens, 2017). A variety of effective flame retardants are now in widespread use, but there are health concerns associated with human exposure. In particular, brominated flame retardants are harmful to human health and as a consequence many of these have been banned or voluntarily phased-out of commercial use (Birnbaum and Staskal, 2004). Polybrominated diphenyl ethers (PBDE) were the primary flame retardant used in residential and office furniture prior to their discontinuation in 2004 when specific congeners were voluntarily phased-out due to their environmental persistence, bioaccumulation, and impairment of neurological development (Birnbaum and Staskal, 2004; Eriksson et al., 2001; Viberg et al., 2002). Organophosphate flame retardants (OPFR) replaced PBDEs as the primary commercial flame retardant, and while there are several OPFRs in use, tris(1, 3-dichloro-2-propyl) phosphate (TDCPP) is perhaps the most widely used (Stapleton et al., 2012; Wang et al., 2019b). TDCPP is sprayed onto polyurethane foams that are used for seating in homes, offices, and vehicles (Stapleton et al., 2009; van der Veen and de Boer, 2012). The TDCPP is not bound to the foams and off-gasses resulting in human exposure (Cequier et al., 2015; van der Veen and de Boer, 2012). Despite its widespread use, it is unclear whether exposure to TDCPP adversely impacts human health.

Epidemiological studies from the National Health and Nutrition Examination Survey (NHANES) correlated urinary OPFR metabolite levels to metabolic syndrome (MetS) and each of the MetS components (Luo et al., 2020). Only metabolites of tris(2-chloroethyl) phosphate and TDCPP showed positive associations with MetS, and the association was specifically in males. Although no single MetS component showed an association with TDCPP exposure, the exposure relationship identified using multivariate models was largely derived from MetS components most associated with insulin resistance, i.e. hyperglycemia and central adiposity. Interestingly, there was a dose-specific negative association between TDCPP exposure and hyperglycemia in females indicating the possibility of sexually dimorphic effects (Luo et al., 2020). It remains to be determined whether TDCPP causes metabolic disruption or is simply associated with behaviors that promote MetS. For example, because TDCPP is used for indoor seating, it is possible that TDCPP exposure is simply a consequence of a sedentary lifestyle.

Rodent studies support OPFR-induced metabolic disruption (Krumm et al., 2018; Wang et al., 2019a). However, in the study testing TDCPP only, the TDCPP concentration (125–500 mg/kg/day) far exceeds estimated human exposure levels (0.02 mg/kg/day). Experiments

by Krumm et al. used doses much closer to human exposure level (1 mg/kg/day) and showed male-sex specific hyperglycemia without increased adiposity or insulin resistance (Krumm et al., 2018). However, because the study used an OPFR mixture, it is unclear whether TDCPP contributed to the observed phenotype. In the present study, TDCPP was incorporated into low phytoestrogen diets at concentrations that include the estimated human exposure dose (0.02 mg/kg/day), the 1 mg/kg/day dose used by Krumm et al., as well as a dose of 100 mg/kg/day, which is near the established lowest observable effect limit of 62 mg/kg/day (Chemicals, 1998). We performed body composition analysis and determined the impact of TDCPP exposure on glucose homeostasis. Finally, to elucidate mechanisms of potential metabolic disruption and sex-specific effects, we screened TDCPP for transactivation of 26 nuclear receptors, including the sex hormone receptors.

2. Methods

2.1. Experimental animals

All rodent experiments were approved by the University of Kentucky Institutional Animal Care and Use Committee. C57BL/6J mice were purchased from The Jackson Laboratory at 5 weeks of age. Mice were housed 2–4 mice per cage at temperature of 21 °C, 50 % humidity, and 14:10 light cycle. Mice were given ad libitum access to food and water. Mice acclimatized for 7 days before being sorted into treatment groups with approximately equal body weights. TDCPP (Santa Cruz Biotechnology, Dallas, TX) was incorporated into a purified low phytoestrogen base diet (TD.95092, Envigo, Indianapolis, IN). Diets contained 0.1 % DMSO (Sigma, Burlington, MA) supplemented with either 0.00 mg TDCPP/kg (Control), 0.166 mg TDCPP/kg, 8.31 mg TDCPP/kg, or 831 TDCPP/kg corresponding to estimated dietary TDCPP intake of 0.0 mg/kg body weight/day, 0.02 mg/kg body weight/day 1.0 mg/kg body weight/day, and 100 mg/kg body weight/day, respectively. Food intake and body weights were recorded weekly for each of the 5 weeks of experimental exposure prior to metabolic phenotyping. Mice were maintained on their designated diets for the duration of the study. Researchers conducting body composition analysis, glucose tolerance tests, and insulin tolerance tests were experimentally blinded.

2.2. Urinary BDCPP measurement

After consuming diets for at least 4 weeks, spot urine was collected in non-fasted mice and stored at 4 °C. BDCPP in urine was extracted and analyzed using published methods with minor modifications (Cooper et al., 2011; Hou et al., 2020). Urine samples were transferred into 1.5 mL tubes and spiked with 5 μL of 1 μg/mL BDCPP-d10 (internal standard, IS), and the pH was adjusted by addition of 0.1 mL of 10 mM ammonium acetate (pH=5, adjusted with acetic acid). After vortex-mixing for 1 min, samples were purified using solid phase extraction (Strata-X-AW, 30 mg, 1 mL cartridge, Phenomenex). The SPE cartridge was conditioned with 1 mL of methanol and 1 mL of pure water. After loading the sample, cartridges were rinsed with 1 mL of water and the analyte was eluted with 1 mL of 5 % pyrrolidine in acetonitrile, and the eluate was collected in 4 mL vials and concentrated under a gentle stream of nitrogen to near dryness and reconstituted with 0.2 mL of water-methanol (4:1). BDCPP analysis was performed on an AB Sciex 4000 Q Trap coupled with an Exion LC system. The Analyst software package was used for data

collection and analysis. Chromatography was carried out with a C_8 reverse-phase column (Waters ACQUITY UPLC BEH C_8, 2.1 × 50 mm, 1.7 μm) maintained at 40 °C and the flow rate was 0.4 mL/min. Mobile phase A and B consisted of 0.1 % formic acid in water and 0.1 % formic acid in methanol. A gradient program was used as follows: (T min/ %A): 0/80, 4.0/5, 8.0/5, 8.1/80, 10.5/80. The injection volume was 5.0 μL. The mass spectrometer was equipped with an electrospray ionization (ESI) source and operated in positive mode under the following operating parameters: IonSpray Voltage 4.5 kV, Desolvation temperature 400 °C, Ion Source Gas 1 40 psi, Ion Source Gas 2 30 psi, Curtain Gas 40 psi, Collision Gas Medium, Entrance Potential 10.0 V, and CXP 10 V. Quantitative analysis was conducted by monitoring the precursor ion to product ion transitions of *m/z* 321.1/99.1 (BDCPP, DP 85 V and CE 28.0 V) and 321.1/209.2 (BDCPP, DP 80 V and CE 16.0 V), *m/z* 331.2/101.2 (BDCPP-d10, DP 80 V and CE 32.0 V), with a dwell time of 0.15 s. In this study, two ion transitions were selected: *m/z* 321.1→99.1 was used for quantitation and *m/z* 321.1→209.2 as confirmation. Standard samples spiked in control urine were prepared as described above with concentrations of 10, 25, 50, 100, 200, and 1000 ng/mL and then quantitation was conducted using corresponding standard curves using Sciex MultiQuant software.

2.3. Body composition analysis

During the fifth week of dietary TDCPP exposure, body weight was recorded and fat mass and lean mass were quantified by nuclear magnetic resonance relaxometry using the EchoMRI-100 (Echo Medical Systems, Houston, TX).

2.4. Glucose tolerance test (GTT)

Male and female mice were fasted 6 h beginning when the lights turned on in the animal housing room (0600 h) to control for the circadian rhythm. Mice were then intraperitoneally injected with sterilefiltered D-glucose (Sigma, Burlington, MA) dissolved in PBS. Blood was sampled from the tail vein at 0, 15, 30, 60 and 120 min after glucose injection. Blood glucose was measured using AlphaTRAK 2 Glucose Monitoring System (Zoetis, Kalamazoo, MI).

2.5. Insulin tolerance test (ITT)

Mice were allowed to recover from the GTT for 48–72 h prior to insulin tolerance testing. Mice were fasted for 4 h beginning at 0600 h. Female mice were intraperitoneally injected with sterile-filtered 0.75 IU/kg regular human insulin (Lilly) diluted in PBS. In separate cohorts, male mice were injected with either 1 or 0.75 IU insulin/kg body weight. Blood glucose was measured via tail venipuncture at 0, 15, 30, 60 and 120 min after insulin injection using AlphaTRAK 2 glucometer. Mice were rescued with an injection of D-glucose and removed from remainder of the procedure if excessive lethargy, seizures, or blood glucose levels below 20 mg/dL were observed.

2.6. Fasting plasma collection

After 7 days recovery from ITT, mice were fasted for 4 h beginning at 0600 h. Mice were punctured in the submandibular vein using a Goldenrod Animal Lancet (Medipoint, Mineola, NY). Approximately 50 μL whole blood was collected into BD Microtainer tubes

with K_2EDTA (Becton, Dickinson and Company, Franklin Lakes, NJ) and 5 μL blood sampled to measure fasting blood glucose levels using AlphaTrak2 glucometer. Blood was centrifuged at 2100 g for 15 min at 4 °C. Plasma was stored at − 80 °C for later quantification of fasting insulin levels. Ultra-Sensitive Mouse Insulin ELISA Kits (Crystal Chem, Elk Grove Village, IL) were used to quantify plasma insulin levels. HOMA-IR was calculated as the product of fasting glucose (mmol/L) and fasting insulin (μIU/mL) divided by 22.5. HOMA-B was calculated as the product of 20 x fasting insulin (μIU/mL) divided by fasting glucose (mmol/L) minus 3.5.

2.7. Terminal tissue collection

Male and female mice were weighed and euthanized via CO_2 asphyxiation after 10 or 11 weeks on TDCPP diets, respectively. Livers and testes were excised and weighed. Gonadal white adipose tissue (WAT) was collected but not weighed. All tissues were stored at − 80 °C for later use.

2.8. Quantification of adipocyte size

Frozen WAT was placed in 10 % formalin at 4 °C for 48 h for fixation as previously described (Laforest et al., 2018). Following ethanol dehydration, WAT was paraffin embedded, sectioned, and H&E staining was performed. Sections were viewed on Nikon Eclipse 80*i* under 10X magnification. Thresholding was performed using Nikon's analysis software, NIS-Elements AR. Cells were selected based on a diameter between 40 and 100 μm and a circularity index between 0.3 and 1. Objects that fell below an area of $350 \mu m^2$ were removed from the sample and empirical cumulative distribution functions (ECDF) of the adipocytes were computed under three different levels of TDCPP exposure (i. e., of 0.0 mg/kg/day,1.0 mg/kg/day, and 100 mg/kg/day). The benefit of using ECDF rather than a binned frequency distribution with $500 \mu m^2$ increments includes the retention of the initial area information and the ability to study variation in overall area by exposure level with greater precision.

2.9. RNA extraction and relative mRNA quantitation

Total RNA from liver tissue was isolated using Pure Link Mini Kit (ThermoFisher Scientific, Waltham, MA) following the manufacture's protocol. RNA quality and concentration were measured on Nanodrop 2000 UV-Vis Spectrophotometer (ThermoFisher, Waltham, MA).

Each sample was diluted to 100 ng/μL and cDNA was synthetized from 0.4 μg RNA with qScript cDNA Supermix (Quanta Biosciences, Beverly, MA) according to manufacturer's instructions. RT-qPCR was conducted with TaqMan Fast Advanced Master Mix (ThermoFisher, Walthman, MA), and the Taqman Gene Expression Assays (ThermoFisher, Walthman, MA) in Table 1. Relative gene expression was determined using the ΔC_T method. Briefly, target gene expression relative to the endogenous control was determined for each sample using the equation $2(^{C_T(Actb)-C_T(Target)})$. Next, the relative gene expression in the Control group was averaged to obtain a calibrator value. Each sample's relative gene expression was then divided by the calibrator to obtain a relative quotient for each target.

2.10. Nuclear receptor transactivation

Nuclear receptor activity was evaluated in vitro by Indigo Biosciences (State College, PA) using Reporter Cells expressing human nuclear receptors, except for mCAR and mPXR which expressed murine receptors. Androgen receptor, estrogen receptor α, estrogen receptor β, glucocorticoid receptor, mineralocorticoid receptor, and progesterone receptor Reporter Cells expressed the native nuclear receptor, and their genetic response elements contained the native promotor sequence functionally linked to luciferase. For all other Reporter Cells, hybrid receptors were used in which the native N-terminal DNA binding domain (DBD) was replaced with the yeast Gal4 DBD. In the hybrid cells, the Gal4 upstream activating sequence was functionally linked to luciferase. Reporter Cell suspensions were seeded onto 96 well plates. Cells were treated with 1 nM, 0.1 μM or 10 μM TDCPP (n = 3) or 0.1 % DMSO vehicle (n = 6). Treated Reporters Cells were incubated for 24 h at 37 °C and 5 % CO_2. Media was replaced with luciferase detection reagent and after 10 min, relative luminescence units (RLU) were recorded to determine nuclear receptor activity. For nuclear receptor antagonist studies, reference agonists were added to Reporter Cell suspension with or without 10 μM TDCPP. After 22 h incubation, media was replaced with luciferase detection reagent and RLU quantified after 10 min. Nuclear receptor activation and inhibition studies used reference agonists and antagonists, respectively, for positive controls. For select Reporter Cells (AR, ERα, LXRβ, PPARα, RARβ, RXRα, and VDR), Live Cell Multiplex Assays (LCMA: Indigo Biosciences) were performed to determine whether TDCPP caused cytotoxicity, which could confound antagonism results. LCMA uses cell-permeate fluorogenic substrate Calcein-AM to assess cell viability with staurosporine used as a positive control. For these studies, after 22 h incubation with reference agonist and 10 μM TDCPP, media was discarded, rinsed with LCMA Buffer, and LCMA Reagent added to cells. After 45 min incubation, fluorescence was quantified. Cells were rinsed again and luciferase detection reagent added for 10 min after which Reporter Cell luminescence was measured to determine nuclear receptor activation.

2.11. Statistical analysis

One-way Analysis of Variance (ANOVA) was performed within each sex with post-hoc Dunnett's to correct for multiple testing. If data failed Brown-Forsythe equal variance test or D′Agostino and Pearson normality test, then One-way ANOVA was performed on log-transformed data. If transformed data failed either equal variance or normality test, then data were analyzed On Ranks. GraphPad Prism 8 was used for these tests and generating figures. GTT and ITT data were analyzed by Repeated measures ANOVA using SigmaPlot. For in vitro nuclear receptor transactivation, we fitted a One-way ANOVA model for each of the 26 nuclear receptors using R statistical software program (R Development Core Team, 2021). To test for an effect of dose on receptor activation, we compared each treatment to the control group. P-values were adjusted according to the False Discovery Rate (FDR) to correct for multiple comparisons. For antagonist studies which only used 1 concentration of TDCPP, we performed T-tests with Bonferroni-Hochberg correction for multiple testing. To test for an effect of dose on the adipocyte area distributions we used the Kolmogorov-Smirnov (K-S) test that measures the compatibility between the empirical distributions of different populations.

3. Results

3.1. TDCPP exposure

Mice were group housed 2–4 mice per cage, therefore, food consumption for the cage was taken as a function of total mouse weight within a given cage. A total of 3 cages of mice per treatment were used in these studies. There was not a treatment effect on food intake in males ($p = 0.083$) or females ($p = 0.441$) (Fig. 1A). Based upon the average dietary intake over the course of 5 weeks on the TDCPP diets, male mice were calculated to consume 0.00 mg/kg/day, 0.02 mg/kg/day, 0.98 mg/kg/day and 99.14 mg/kg/day. Females on average consumed 0.00 mg/kg/day, 0.02 mg/kg/day, 1.08 mg/kg/day, and 112 mg/kg/day. These values are very close to the target doses of 0.00, 0.02, 1, and 100 mg/kg/day. BDCPP is the primary metabolite of TDCPP, and we measured BDCPP levels in the urine. BDCPP levels were below the limit of detection (LOD = 2 ng/mL) in Control group. As expected, the 0.02 mg/kg/day dose reproduced urinary BDCPP levels that were close to the maximum level of ~ 200 ng/mL observed in human populations (Boyle et al., 2019). Regression analysis indicates that dietary TDCPP exposure of 0.3 μg/kg/day would produce urinary levels of approximately 1.7 ng/mL, which is representative of the general adult American population (Boyle et al., 2019). Urinary BDCPP levels were 50-fold higher in mice exposed to 1 mg/kg /day compared to mice exposed to 0.02 mg/kg/day, which mirrors the 50-fold increase in dietary exposure. Mice exposed to 100 mg/kg/day produced average urinary BDCPP levels of 355,000 ng/mL, which is a 50-fold increase from urinary BDCPP levels of mice exposed to 1 mg/kg/day. This deviates from the expected 100-fold increase that was expected due to the 100-fold increase in dietary exposure. The cause of reduced urinary BDCPP levels may result from saturation of TDCPP metabolism and BDCPP urinary elimination, thus skewing the elimination toward other known routes, such as fecal excretion. Feces were not collected, therefore, we are unable to confirm this explanation.

3.2. TDCPP-induced adiposity

Body composition analysis was performed during the fifth week of TDCPP diet consumption. In males, there was no difference in body weight between treatment groups (Fig. 2A: $p = 0.633$), however, percent body fat was increased ($p = 0.016$), and percent lean mass was decreased in the 1 mg/kg and 100 mg/kg groups compared to Controls ($p = 0.005$) (Fig. 2B). Furthermore, the fat mass to lean mass ratio was increased in males in the 1 mg/kg and 100 mg/kg groups (Fig. 2B: $p = 0.015$). Gonadal WAT was sectioned and stained to quantify adipocyte size in males. There was a difference in the ECDF distributions of adipocyte area by TDCPP exposure (Supplemental Fig. 1: $p < 0.001$). Males in the 1 mg/kg and 100 mg/kg groups had more adipocytes with area that fall above $4500 \mu m^2$ relative to the Controls. Contrary to the TDCPP-induced adiposity in males, no effect of TDCPP on body weight (Fig. 2C: $p = 0.840$), percent body fat (Fig. 2D: $p = 0.496$), percent lean mass ($p = 0.242$), or fat mass to lean mass ratio ($p = 0.468$) were observed in females. Taken together, these data indicate that TDCPP causes dose-dependent alterations in body composition that favors metabolic disruption only in males.

3.3. TDCPP-induced metabolic disruption

Intraperitoneal glucose tolerance tests revealed no significant difference in glucose tolerance in males (Fig. 3A: $p = 0.211$). Although the incremental area under the curve for the male GTT was statistically significant ($p = 0.045$), there was not a TDCPP experimental group that differed from vehicle-exposed Control mice. Insulin tolerance tests showed that male mice exposed to 100 mg TDCPP/kg/day have whole body insulin resistance (Fig. 3B: $p = 0.013$). Glucose levels only declined 20 % in response to insulin whereas the Control group declined 50 %. Males also displayed fasting hyperglycemia (Fig. 3C: $p = 0.017$) with the 100 mg TDCPP/kg/day group being most affected (Dunnett's $p = 0.056$), but fasting insulin levels were comparable between treatment groups (Fig. 3C: $p = 0.636$). Using the fasting glucose and insulin levels, we calculated the HOMA-IR for insulin resistance and HOMA-B for β-cell function, but neither showed an effect of TDCPP exposure (Fig. 3C: $p = 0.779$ and $p = 0.151$, respectively). In contrast to TDCPP-induced insulin resistance and fasting hyperglycemia observed in males, female mice were resistant to metabolic disruption. Compared to female vehicle-exposed mice, female mice exposed to TDCPP showed comparable glucose tolerance (Fig. 3D: $p = 0.450$), incremental glucose area under the curve ($p = 0.278$), insulin sensitivity (Fig. 3E: $p = 0.750$), fasting glucose (Fig. 3F: $p = 0.120$), fasting insulin ($p = 0.957$), HOMA-IR ($p = 0.977$) and HOMA-B ($p = 0.551$). Thus, TDCPP disrupts glucose homeostasis specifically in males by attenuating insulin sensitivity.

3.4. TDCPP effects on nuclear receptor activation

To elucidate mechanisms by which TDCPP causes metabolic disruption, we screened TDCPP for agonist activity against 26 nuclear receptors and for antagonist activity against 18 nuclear receptors. TDCPP did not activate nuclear receptors at concentrations of 1.0 nM or 0.1 μM. However, TDCPP at 10 μM caused significant changes in reporter gene activation compared to Reporter Cells exposed to Vehicle (Table 2). Significant nuclear receptor transactivation was revealed for mCAR, PPARγ, RXRβ, FXR, PXR, and mPXR, but only the latter 3 were activated at least 2-fold compared to Controls. TDCPP exposure at 10 μM caused a 2.5-fold increase in human FXR activation (q = 6.61e-9), 17-fold increase in human PXR activation (q = 1.71e-16), and a 16-fold increase in mouse PXR activation (q = 6.82e-17). Human and mouse PXR activation was 57 % and 94 % relative to 30 μM PXR reference agonists Rifampicin and PCN, respectively, indicating robust activation. TDCPP-induced antagonism was observed for AR, FXR, and RXRβ (Table 2). Although these were statistically significant, only AR activity was inhibited ≥ 50 % signifying potential physiologically relevant antagonism. Of note, TDCPP exposure caused 45 % inhibition of ERβ, but did not reach statistical significance (q = 5.68E-2).

FXR and PXR nuclear receptors are expressed primarily in the liver, therefore, we quantified relative gene expression of FXR, PXR, and genes regulated by these nuclear receptors in the liver. After 10 weeks on TDCPP diets, TDCPP did not affect gene expression of FXR or PXR (Fig. 4). However, the 100 mg TDCPP/kg/day caused differential hepatic gene expression of PXR-target genes *Cyp3a11* and *Gstm3*. *Cyp3a11* expression was increased 4.6-fold ($p < 0.001$) in male livers and 1.7-fold in female livers ($p < 0.001$). *Gstm3* was increased 2.5-fold ($p = 0.013$) in male livers and 2.7-fold ($p < 0.001$) in female livers. To support anti-androgen activity of TDCPP in male mice, we measured testes weight after

10 weeks on TDCPP diets, but there was no difference between treatment groups (data not shown).

4. Discussion

Epidemiological studies have uncovered a positive association with TDCPP exposure and MetS, and this effect is predominantly associated with the MetS components hyperglycemia and central obesity (Luo et al., 2020). Because insulin resistance is closely associated with these two MetS components, the current study was conducted to determine whether a causal relationship exists between TDCPP exposure and perturbations in glucose homeostasis. By incorporating TDCPP into the rodent diet, we show that dietary TDCPP exposure engenders adiposity, insulin resistance, and fasting hyperglycemia in male mice. Consistent with observations in humans, female mice were protected from TDCPP-induced metabolic perturbations.

A range of doses were used including the dose of 0.02 mg TDCPP/kg/day, which is the estimated level of human exposure. Indeed, our studies show this dose in C57BL/6J mice results in urinary BDCPP levels at the upper limits reported in humans (Boyle et al., 2019). However, we did not detect any perturbations related to adiposity or glucose homeostasis at this exposure level. Of course, humans are subject to more prolonged exposure to TDCPP as well as many other environmental factors that contribute, in varying degrees, to metabolic disruption. Perhaps further challenging mice with macronutrient dense Western Diet would uncover defects in glucose homeostasis at TDCPP-exposure levels that more closely reflect human exposure, but this remains to be determined. Mice treated with 1 mg TDCPP/kg/day exhibited male sex-specific adiposity without impairment in glucose homeostasis. Other studies show that oral exposure to OPFR mixture consisting of 1 mg/kg each of TDCPP, triphenyl phosphate, and tricresyl phosphate for 4 weeks caused fasting hyperglycemia in males but did not affect adiposity (Krumm et al., 2018). The inclusion of the non-chlorinated OPFR likely explains the differences between our two studies. As it stands, it was the 100 mg/kg/day dose that caused metabolic disruption. Although this dose far exceeds human exposure level, it reproduces the male sex-specific insulin resistance associated with exposure in humans and provides a mouse exposure model where interventions can be tested in the future.

TDCPP exposure failed to impair glucose tolerance during GTT in male mice, but resulted in fasting hyperglycemia and insulin resistance during ITT. Typically with obesity, fasting hyperglycemia and insulin resistance are associated with fasting hyperinsulinemia, but this was not the case as fasting insulin levels were unaffected. Because insulin levels were not reflective of insulin resistance, HOMA-IR and HOMA-B were comparable between treatment groups. Thus, it would appear TDCPP-induced adiposity is not mediating the disruption in glucose homeostasis. Decreased β-cell function would explain the lack of fasting hyperinsulinemia, but decreased β-cell function with concomitant insulin resistance would combine to cause moderate to severe glucose intolerance during the GTT. Because glucose tolerance was normal in males despite insulin resistance, it is likely the case that 100 mg TDCPP/kg/day is not causing β-cell dysfunction, but rather, TDCPP is causing hepatic insulin resistance. Future studies will employ hyperinsulinemic-euglycemic clamp

in TDCPP-exposed mice to reveal the defect in insulin action leading to diminished insulin-mediated glucose lowering. In our study, metabolic disruption caused by dietary TDCPP exposure was male sex-specific, which agrees with epidemiological findings.

There are many mechanisms by which xenobiotics cause sex-specific effects or metabolic disruption (Heindel et al., 2017). We interrogated nuclear receptors as possible mediators of the observed phenotypes because endocrine disruption of sex hormone nuclear receptors AR, ERα, and ERβ may facilitate sex differences (De Paoli et al., 2021; Muller et al., 2005; Navarro et al., 2015). Moreover, other nuclear receptors such as LXR, PPARs, TR, GCR, and VDR have roles in macronutrient metabolism, which can influence insulin sensitivity and type 2 diabetes risk (Dixit and Prabhu, 2022; Dixon et al., 2021; Huang et al., 2013; Kokkinopoulou et al., 2021; Palomer et al., 2008). For some nuclear receptors, activation is associated with metabolic disruption, while for others, it is decreased activity that is associated with impaired metabolism. For instance, xenobiotic activation of estrogen receptors can cause obesity and insulin resistance (Provvisiero et al., 2016), while diminished PPAR activity can cause insulin resistance (Tsai et al., 2009). Therefore, in vitro studies for both TDCPP-induced nuclear receptor activation and inhibition were conducted. FXR was activated by TDCPP in vitro, but we did not find transcriptional evidence of FXR activation in mouse livers. As FXR activation is generally protective against impaired glucose tolerance (Gonzalez-Regueiro et al., 2017; Li et al., 2020; Shapiro et al., 2018), it was not expected that FXR-regulated genes would be differentially expressed in TDCPP-exposed livers, especially in insulin resistant males. The xenobiotic nuclear receptor, PXR, was activated most robustly, and this was confirmed by gene expression analysis is livers of both male and female mice exposed to TDCPP. Importantly, while many PXR agonists are species specific (Krasowski et al., 2005), TDCPP activated both mouse and human PXR to similar extents, further qualifying our mouse model for the study of health effects associated with TDCPP exposure. PXR activation causes insulin resistance in humans and rodents (Rysa et al., 2013; Zhou, 2016), and PXR ablation alleviates metabolic disruption in obese and diabetic mice (He et al., 2013). Interestingly, our data support TDCPP-induced PXR activation in both male and female mice despite adverse phenotypes being male sex-specific. This may be due to the established protective effect of estrogen in females (De Paoli et al., 2021; Mauvais-Jarvis et al., 2013) or sexually dimorphic effects of downstream of PXR (Gong et al., 2006).

Our data also show that TDCPP is an anti-androgen in vitro, which is consistent with other studies (Kojima et al., 2013; Kojima et al., 2016). PXR agonist, rifampicin, exerts anti-androgen effects via PXR-mediated upregulation of androgen metabolizing enzymes Cyp3a and Sult2a1 (Zhang et al., 2010). Dexamethasone is an alternative positive control in PXR activation studies. Dexamethasone is an AR antagonist through direct binding to the AR rather than androgen metabolism (Park et al., 2021). In the present study, 5-alpha-dihydro-11-keto testosterone was used as the AR reference agonist. Its susceptibility to PXR-mediated metabolism is unknown, therefore, it is likewise unknown whether TDCPP's AR antagonism is via direct interaction with the receptor or via metabolism of the reference agonist. Regardless of its antagonism mechanism, TDCPP's anti-androgen activity potentially contributes to metabolic disruption associated with exposure. Androgen deficiency in males is associated with increased adiposity and decreased lean mass (Navarro

et al., 2015; Singh et al., 2003), which we observe in our mouse model. However, we did not find a difference is relative testes weight even after 10 weeks on TDCPP diets, supporting that TDCPP is not causing systemic anti-androgen effects. Because TDCPP is readily metabolized by the liver, it may be that TDCPP's anti-androgen effects are confined to the liver. Genetic ablation of AR activity specifically in the liver exacerbates obesity, insulin resistance, and impaired glucose tolerance in male mice challenged with high fat feeding (Lin et al., 2008). However, without the challenge of over nutrition, liver-specific AR knockout males have no impairment in glucose homeostasis (Lin et al., 2008), suggesting that TDCPP-induced AR antagonism is likely not the mechanism of sex-specific insulin resistance. However, to be certain, additional studies interrogating AR activity in TDCPP-exposed mice are needed to determine whether TDCPP is acting as an anti-androgen in our mouse model, and further, to determine whether AR antagonism is the mechanism leading to TDCPP-induced insulin resistance.

While this study is not the first to show in vitro that TDCPP is a PXR agonist and AR antagonist, we are the first to investigate nearly all the nuclear receptors for agonist and antagonist activity and extrapolate our findings to a mammalian animal model. Studies have suggested that OPFR modulates thyroid function or estrogen activity (Krumm et al., 2018; Meeker and Stapleton, 2010), but our in vitro studies do not support a direct action of TDCPP on these nuclear receptors although we cannot exclude the possibility of indirect effects. Moreover, other OPFR or xenobiotics may contribute to the associated thyroid and estrogen disruption in those studies. Although we focused our investigation on TDCPP-induced modulation of nuclear receptors, there are other potential mechanisms by which TDCPP can cause insulin resistance such as TDCPP-induced mitochondrial dysfunction (Kim et al., 2008; Le et al., 2021; Lee et al., 2019; Marroqui et al., 2018). The mechanisms by which TDCPP causes metabolic syndrome in men remains to be determined, and may include modulation of nuclear receptors, mitochondrial dynamics, and others yet to be uncovered.

Herein, we have described a mouse model of TDCPP exposure that reproduces sex-specific maladies associated with human exposure. Future studies using this preclinical exposure model should explore, among other potential mechanisms, the metabolic sequelae associated with TDCPP-induced modulation of PXR and AR nuclear receptors and the protective role of estrogens to elucidate the mechanism(s) by which TDCPP causes male-sex specific adiposity and insulin resistance.

Supplementary Material

Refer to Web version on PubMed Central for supplementary material.

Funding

This publication was supported in part by UK-Center for Appalachian Research in Environmental Sciences (P30 ES026529) and the Institutional Development Award (IDeA) from NIGMS (P30 GM127211). This publication and its contents are solely the responsibility of the authors and do not necessarily represent the official views of the NIH.

Data Availability

Data will be made available on request.

References

Ahrens M, 2017. Trends and Patterns of U.S. Fire Losses.

Birnbaum LS, Staskal DF, 2004. Brominated flame retardants: cause for concern? Environ. Health Perspect 112, 9–17. [PubMed: 14698924]

Boyle M, Buckley JP, Quiros-Alcala L, 2019. Associations between urinary organophosphate ester metabolites and measures of adiposity among U.S. children and adults: NHANES 2013-2014. Environ. Int 127, 754–763. [PubMed: 31003058]

Cequier E, Sakhi AK, Marce RM, Becher G, Thomsen C, 2015. Human exposure pathways to organophosphate triesters - a biomonitoring study of mother-child pairs. Environ. Int. 75, 159–165. [PubMed: 25461425]

Chemicals, I.-O. PftS.Mo, 1998. Flame retardants: tris(chloropropyl) phosphate and tris (2-chloroethyl) phosphate. In: Organization, W.H. (Ed.).

Cooper EM, Covaci A, van Nuijs AL, Webster TF, Stapleton HM, 2011. Analysis of the flame retardant metabolites bis(1,3-dichloro-2-propyl) phosphate (BDCPP) and diphenyl phosphate (DPP) in urine using liquid chromatography-tandem mass spectrometry. Anal. Bioanal. Chem 401, 2123–2132. [PubMed: 21830137]

De Paoli M, Zakharia A, Werstuck GH, 2021. The role of estrogen in insulin resistance: a review of clinical and preclinical data. Am. J. Pathol 191, 1490–1498. [PubMed: 34102108]

Dixit G, Prabhu A, 2022. The pleiotropic peroxisome proliferator activated receptors: regulation and therapeutics. Exp. Mol. Pathol 124, 104723. [PubMed: 34822814]

Dixon ED, Nardo AD, Claudel T, Trauner M, 2021. The role of lipid sensing nuclear receptors (PPARs and LXR) and metabolic lipases in obesity, diabetes and NAFLD. Genes 12.

Eriksson P, Jakobsson E, Fredriksson A, 2001. Brominated flame retardants: a novel class of developmental neurotoxicants in our environment? Environ. Health Perspect 109, 903–908. [PubMed: 11673118]

Gong H, Singh SV, Singh SP, Mu Y, Lee JH, Saini SP, Toma D, Ren S, Kagan VE, Day BW, Zimniak P, Xie W, 2006. Orphan nuclear receptor pregnane X receptor sensitizes oxidative stress responses in transgenic mice and cancerous cells. Mol. Endocrinol 20, 279–290. [PubMed: 16195250]

Gonzalez-Regueiro JA, Moreno-Castaneda L, Uribe M, Chavez-Tapia NC, 2017. The role of bile acids in glucose metabolism and their relation with diabetes. Ann. Hepatol 16, 16–21.

He J, Gao J, Xu M, Ren S, Stefanovic-Racic M, O'Doherty RM, Xie W, 2013. PXR ablation alleviates diet-induced and genetic obesity and insulin resistance in mice. Diabetes 62, 1876–1887. [PubMed: 23349477]

Heindel JJ, Blumberg B, Cave M, Machtinger R, Mantovani A, Mendez MA, Nadal A, Palanza P, Panzica G, Sargis R, Vandenberg LN, Vom Saal F, 2017. Metabolism disrupting chemicals and metabolic disorders. Reprod. Toxicol 68, 3–33. [PubMed: 27760374]

Hou M, Shi Y, Jin Q, Cai Y, 2020. Organophosphate esters and their metabolites in paired human whole blood, serum, and urine as biomarkers of exposure. Environ. Int 139, 105698. [PubMed: 32278199]

Huang YY, Gusdon AM, Qu S, 2013. Cross-talk between the thyroid and liver: a new target for nonalcoholic fatty liver disease treatment. World J. Gastroenterol 19, 8238–8246. [PubMed: 24363514]

Kim JA, Wei Y, Sowers JR, 2008. Role of mitochondrial dysfunction in insulin resistance. Circ. Res 102, 401–414. [PubMed: 18309108]

Kojima H, Takeuchi S, Itoh T, Iida M, Kobayashi S, Yoshida T, 2013. In vitro endocrine disruption potential of organophosphate flame retardants via human nuclear receptors. Toxicology 314, 76–83. [PubMed: 24051214]

Kojima H, Takeuchi S, Van den Eede N, Covaci A, 2016. Effects of primary metabolites of organophosphate flame retardants on transcriptional activity via human nuclear receptors. Toxicol. Lett 245, 31–39. [PubMed: 26778350]

Kokkinopoulou I, Diakoumi A, Moutsatsou P, 2021. Glucocorticoid receptor signaling in diabetes. Int. J. Mol. Sci 22.

Krasowski MD, Yasuda K, Hagey LR, Schuetz EG, 2005. Evolution of the pregnane x receptor: adaptation to cross-species differences in biliary bile salts. Mol. Endocrinol 19, 1720–1739. [PubMed: 15718292]

Krumm EA, Patel VJ, Tillery TS, Yasrebi A, Shen J, Guo GL, Marco SM, Buckley BT, Roepke TA, 2018. Organophosphate flame-retardants alter adult mouse homeostasis and gene expression in a sex-dependent manner potentially through interactions with ERalpha. Toxicol. Sci 162, 212–224. [PubMed: 29112739]

Laforest S, Pelletier M, Michaud A, Daris M, Descamps J, Soulet D, Jensen MD, Tchernof A, 2018. Histomorphometric analyses of human adipose tissues using intact, flash-frozen samples. Histochem. Cell Biol 149, 209–218. [PubMed: 29356964]

Le Y, Shen H, Yang Z, Lu D, Wang C, 2021. Comprehensive analysis of organophosphorus flame retardant-induced mitochondrial abnormalities: Potential role in lipid accumulation. Environ. Pollut 274, 116541. [PubMed: 33529899]

Lee S, Lee H, Kim KT, 2019. Optimization of experimental conditions and measurement of oxygen consumption rate (OCR) in zebrafish embryos exposed to organophosphate flame retardants (OPFRs). Ecotoxicol. Environ. Saf 182, 109377. [PubMed: 31254858]

Li C, Yang J, Wang Y, Qi Y, Yang W, Li Y, 2020. Farnesoid X receptor agonists as therapeutic target for cardiometabolic diseases. Front Pharm. 11, 1247.

Lin HY, Yu IC, Wang RS, Chen YT, Liu NC, Altuwaijri S, Hsu CL, Ma WL, Jokinen J, Sparks JD, Yeh S, Chang C, 2008. Increased hepatic steatosis and insulin resistance in mice lacking hepatic androgen receptor. Hepatology 47, 1924–1935. [PubMed: 18449947]

Luo K, Zhang R, Aimuzi R, Wang Y, Nian M, Zhang J, 2020. Exposure to organophosphate esters and metabolic syndrome in adults. Environ. Int 143, 105941. [PubMed: 32679393]

Marroqui L, Tuduri E, Alonso-Magdalena P, Quesada I, Nadal A, Dos Santos RS, 2018. Mitochondria as target of endocrine-disrupting chemicals: implications for type 2 diabetes. J. Endocrinol 239, R27–R45. [PubMed: 30072426]

Mauvais-Jarvis F, Clegg DJ, Hevener AL, 2013. The role of estrogens in control of energy balance and glucose homeostasis. Endocr. Rev 34, 309–338. [PubMed: 23460719]

Meeker JD, Stapleton HM, 2010. House dust concentrations of organophosphate flame retardants in relation to hormone levels and semen quality parameters. Environ. Health Perspect 118, 318–323. [PubMed: 20194068]

Muller M, Grobbee DE, den Tonkelaar I, Lamberts SW, van der Schouw YT, 2005. Endogenous sex hormones and metabolic syndrome in aging men. J. Clin. Endocrinol. Metab 90, 2618–2623. [PubMed: 15687322]

Navarro G, Allard C, Xu W, Mauvais-Jarvis F, 2015. The role of androgens in metabolism, obesity, and diabetes in males and females. Obesity 23, 713–719. [PubMed: 25755205]

Palomer X, Gonzalez-Clemente JM, Blanco-Vaca F, Mauricio D, 2008. Role of vitamin D in the pathogenesis of type 2 diabetes mellitus. Diabetes Obes. Metab 10, 185–197. [PubMed: 18269634]

Park Y, Park J, Lee HS, 2021. Endocrine disrupting potential of veterinary drugs by in vitro stably transfected human androgen receptor transcriptional activation assays. Environ. Pollut 286, 117201. [PubMed: 33965802]

Provvisiero DP, Pivonello C, Muscogiuri G, Negri M, de Angelis C, Simeoli C, Pivonello R, Colao A, 2016. Influence of Bisphenol A on Type 2 Diabetes Mellitus. Int. J. Environ. Res Public Health 13.

Rysa J, Buler M, Savolainen MJ, Ruskoaho H, Hakkola J, Hukkanen J, 2013. Pregnane X receptor agonists impair postprandial glucose tolerance. Clin. Pharm. Ther 93, 556–563.

Shapiro H, Kolodziejczyk AA, Halstuch D, Elinav E, 2018. Bile acids in glucose metabolism in health and disease. J. Exp. Med 215, 383–396. [PubMed: 29339445]

Singh R, Artaza JN, Taylor WE, Gonzalez-Cadavid NF, Bhasin S, 2003. Androgens stimulate myogenic differentiation and inhibit adipogenesis in C3H 10T1/2 pluripotent cells through an androgen receptor-mediated pathway. Endocrinology 144, 5081–5088. [PubMed: 12960001]

Stapleton HM, Klosterhaus S, Eagle S, Fuh J, Meeker JD, Blum A, Webster TF, 2009. Detection of organophosphate flame retardants in furniture foam and U.S. house dust. Environ. Sci. Technol 43, 7490–7495. [PubMed: 19848166]

Stapleton HM, Sharma S, Getzinger G, Ferguson PL, Gabriel M, Webster TF, Blum A, 2012. Novel and high volume use flame retardants in US couches reflective of the 2005 PentaBDE phase out. Environ. Sci. Technol 46, 13432–13439. [PubMed: 23186002]

Tsai YS, Tsai PJ, Jiang MJ, Chou TY, Pendse A, Kim HS, Maeda N, 2009. Decreased PPAR gamma expression compromises perigonadal-specific fat deposition and insulin sensitivity. Mol. Endocrinol 23, 1787–1798. [PubMed: 19749155]

van der Veen I, de Boer J, 2012. Phosphorus flame retardants: properties, production, environmental occurrence, toxicity and analysis. Chemosphere 88, 1119–1153. [PubMed: 22537891]

Viberg H, Fredriksson A, Eriksson P, 2002. Neonatal exposure to the brominated flame retardant 2,2′,4,4′,5-pentabromodiphenyl ether causes altered susceptibility in the cholinergic transmitter system in the adult mouse. Toxicol. Sci 67, 104–107. [PubMed: 11961222]

Wang S, Hu X, Li X, 2019a. Sub-chronic exposure to Tris(1,3-dichloro-2-propyl) phosphate induces sex-dependent hepatotoxicity in rats. Environ. Sci. Pollut. Res. Int 26, 33351–33362. [PubMed: 31522405]

Wang S, Romanak KA, Hendryx M, Salamova A, Venier M, 2020. Association between Thyroid Function and Exposures to Brominated and Organophosphate Flame Retardants in Rural Central Appalachia. Environ. Sci. Tech 54 (1), 325–334. 10.1021/acs.est.9b04892.

Zhang B, Cheng Q, Ou Z, Lee JH, Xu M, Kochhar U, Ren S, Huang M, Pflug BR, Xie W, 2010. Pregnane X receptor as a therapeutic target to inhibit androgen activity. Endocrinology 151, 5721–5729. [PubMed: 20962047]

Zhou C, 2016. Novel functions of PXR in cardiometabolic disease. Biochim. Biophys. Acta 1859, 1112–1120. [PubMed: 26924429]

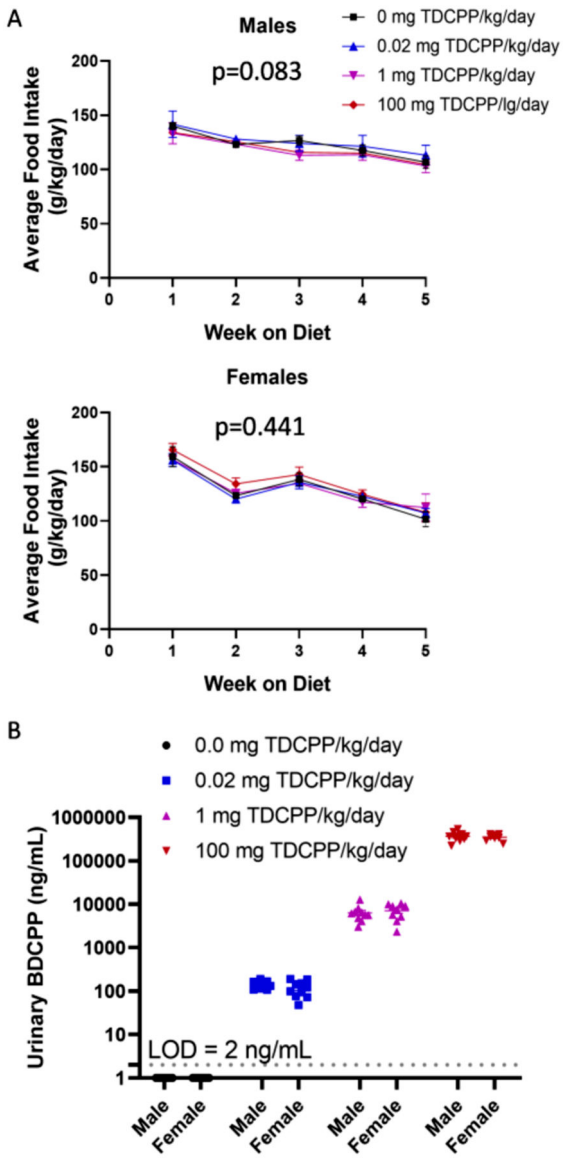

Fig. 1.

TDCPP exposure. A) Mice were group housed according to sex and treatment, and weekly food consumption was recorded for the cage and averaged across body weight. B) After 4 weeks of consuming TDCPP diets, spot urine was collected and BDCPP measured by LC-MS.

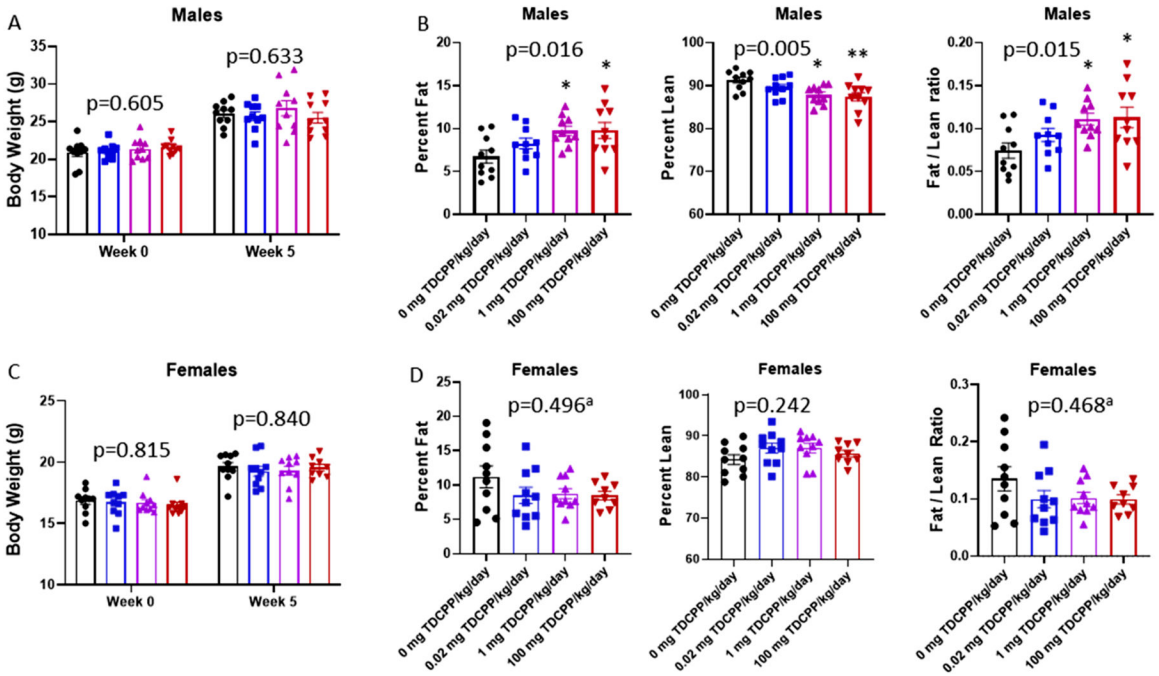

Fig. 2.

Evaluation of TDCPP-induced adiposity. Body weights (A and C) were recorded at baseline and after 5 weeks consumption of TDCPP-containing diets. EchoMRI was used to quantify the proportion of body weight attributed to fat mass and lean mass in males (B) and females (D). 'a′ indicates data were log-transformed for statistical analysis. One-way ANOVA p-values are included in each graph with symbols representing post-hoc analysis. * indicates $p < 0.05$ vs 0 mg TDCPP/kg/day. ** indicates $p < 0.01$ vs 0 mg/kg/day.

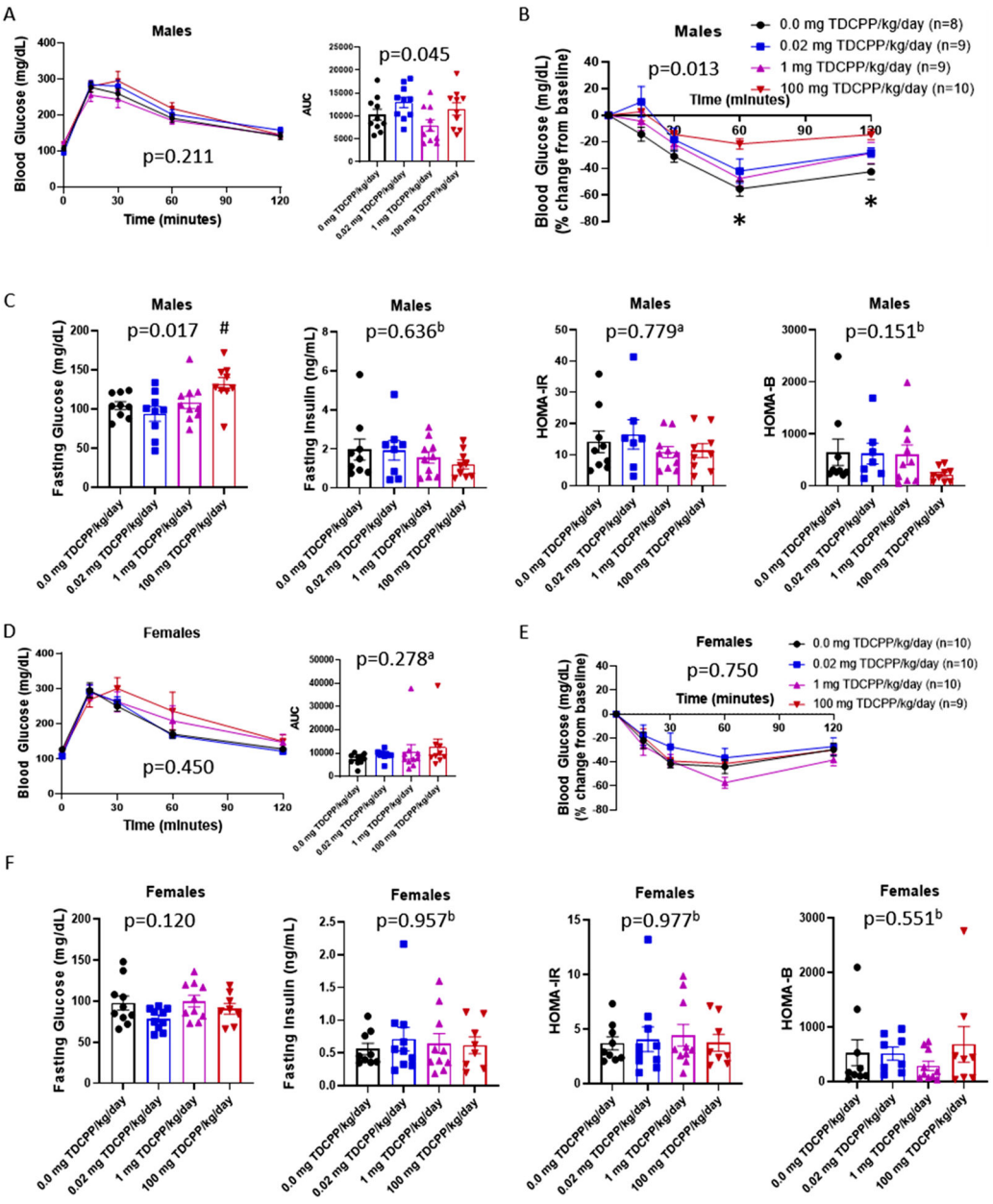

Fig. 3.

Glucose homeostasis in male and female mice. Glucose tolerance tests were performed after 6 h fast and area under the curve calculated (A and D). Insulin tolerance tests were performed after 4 h fast (B and E). Male mice were fasted 4 h and blood glucose levels were recorded and plasma collected for quantification of insulin and subsequent calculation of HOMA-IR and HOMA-B (C and E). ‘a′ indicates data were log-transformed for statistical analysis. One-way ANOVA p-values are included in each graph with symbols representing post-hoc analysis. ‘b′ indicates data were analyzed on Ranks. * indicates $p < 0.05$, 100 mg vs. 0.0 mg TDCPP/kg/day. # indicates $p < 0.06$, 100 mg vs. 0.0 mg TDCPP/kg/day.

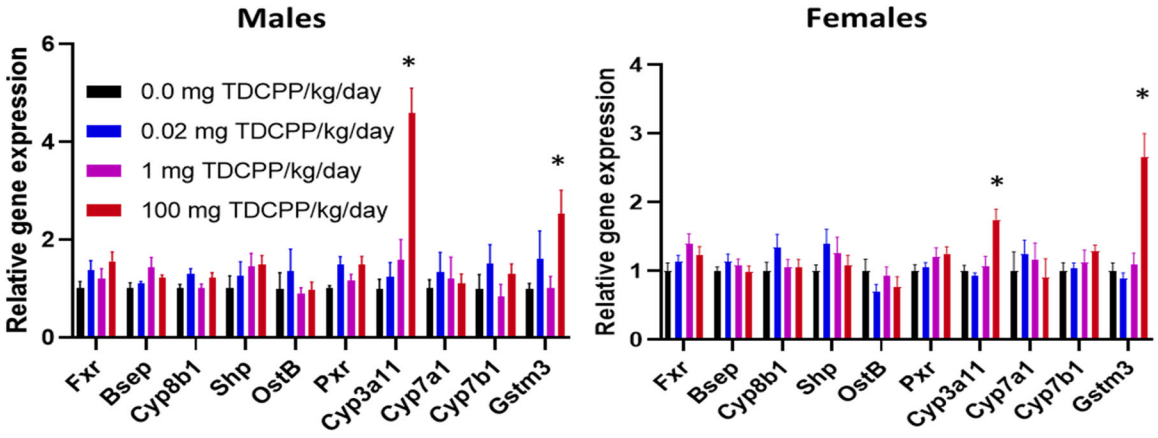

Fig. 4.

TDCPP-induced gene expression in liver. Gene expression of *Fxr*, FXR-regulated genes (*Bsep, Cyp8b1, Shp*, and *Ostβ*), *Pxr* and PXR-regulated genes (*Cyp3a11, Cyp7a1, Cyp7b1*, and *Gstm3*) were quantified by RT-qPCR. n = 5–10. * indicates $p < 0.05$, 100 mg TDCPP/kg/day vs 0.0 mg TDCPP/kg/day.

Table 1

TaqMan Gene Expression Assays.

Gene	Symbol	TaqMan Assay
Beta-actin	*Actb*	Mm00607939
Pregnane X Receptor (Nr1i2)	*Pxr*	Mm01344139
Farnesoid X Receptor (Nr1h4)	*Fxr*	Mm00436425
Small heterodimer parter (Nr0b2)	*Shp*	Mm00442278
Bile salt export pump (Abcb11)	*Bsep*	Mm00445168
Sterol 12-alpha-hydroxylase	*Cyp8b1*	Mm00501637
Organic solute transporter subunit beta (Slc51b)	*Ostβ*	Mm01175040
Cholesterol 7-alpha-hydroxylase	*Cyp7a1*	Mm00484152
cytochrome P450, family 3, subfamily a, polypeptide 11	*Cyp3a11*	Mm00731567
Oxysterol 7-alpha-hydroxylase	*Cyp7b1*	Mm00484157
Glutathione S-Transferase Mu 3	*Gstm3*	Mm00833923

Table 2

Effect of TDCPP on Nuclear Receptor Transactivation *In Vitro*.

Receptor	Host Cell-line	Receptor Form	Reference Agonist	Reference Antagonist	10 μM TDCPP		10 μM TDCPP	
					Fold Activation	q-value	Percent Inhibition	q-value
AR	CV-1	Native	6α Fluoro-testosterone[a]	OH-Flutamide	1.31	NS	80 %	7.00E-06
CAR2	HEK293	Gal4 hybrid	DEHP		1.00	NS		
CAR3	CHO	Gal4 hybrid	CITCO		0.65	NS		
mCAR	CHO	Gal4 hybrid	TCPOBOP		1.51	1.35E-02		
ERα	CHO	Native	17α-Estradiol	Endoxifen	0.41	1.62E-04	14.4 %	NS
ERβ	CHO	Native	17β-Estradiol	PHTPP	1.16	NS	44.7 %	NS
FXR	CHO	Gal4 hybrid	GW4064	DY268	2.50	6.61E-09	26.5 %	7.79E-03
GR	CHO	Native	Dexamethasone		1.08	NS		
LXRα	CHO	Gal4 hybrid	T0901317	GSK2033	0.94	NS	−0.2%	NS
LXRβ	CHO	Gal4 hybrid	T0901317	GSK2033	0.78	2.40E-02	−1.9 %	NS
MR	CHO	Native	Aldosterone		0.80	NS		
PGR	HEK293	Native	Progesterone		0.91	NS		
PPARα	CHO	Gal4 hybrid	GW590735[b]	Not Available	1.09	NS	2.3 %	NS
PPARδ	CHO	Gal4 hybrid	GW0742	GSK3787	0.94	NS	11.7 %	NS
PPARγ	CHO	Gal4 hybrid	Rosiglitazone	T0070907	1.46	2.84E-04	6.1 %	NS
PXR	HEK292	Gal4 hybrid	Rifampicin		17.39	1.71E-16		
mPXR	HEK293	Gal4 hybrid	Pregnenolone-16α-carbonitrile		15.96	6.82E-17		
RARα	CHO	Gal4 hybrid	9-cis-Retinoic acid	BMS195614	0.65	NS	6.5 %	NS
RARβ	CHO	Gal4 hybrid	all trans-Retinoic acid	CD2665	0.61	3.39E-03	15.6 %	NS
RARγ	CHO	Gal4 hybrid	all trans-Retinoic acid	CD2666	1.12	NS	8.8 %	NS
RXRα	CHO	Gal4 hybrid	9-cis-Retinoic acid	UV13003	1.13	NS	6.9 %	NS
RXRβ	CHO	Gal4 hybrid	9-cis-Retinoic acid	UV13003	1.75	6.16E-07	27.9 %	3.75E-02
RXRγ	CHO	Gal4 hybrid	9-cis-Retinoic acid	UV13003	0.80	2.64E-02	22.6 %	NS
TRα	HEK293	Gal4 hybrid	T3	Not Available	0.85	NS	7.6 %	NS
TRβ	HEK293	Gal4 hybrid	T3	Not Available	1.15	NS	11.9 %	NS
VDR	HEK293	Gal4 hybrid	Calcitriol	Not Available	0.38	1.47E-02	7.3 %	NS

Blank cells indicate nuclear receptors for which TDCPP was not tested for antagonism NS: Not Significant (q > 0.05)

[a]: 5α-Dihydro-11-keto testosterone was used as reference agonist for antagonist studies

[b]: GW7647 was used as reference agonist for antagonist studies